Observations of Energetic High-Wavenumber Internal Waves in the Kuroshio

LUC RAINVILLE AND ROBERT PINKEL
Marine Physical Laboratory, Scripps Institution of Oceanography.

(Manuscript received 10 March 2003, in final form February 2004)

ABSTRACT

Intense and spatially coherent shear layers were detected in and under the Kuroshio in an April 2000 (ASIAEX) survey in the East China Sea. The sloping layers, revealed by shipboard Doppler sonars on the R/V *Roger Revelle*, appeared to cross isopycnal surfaces. Except in a small region near the Kuroshio shelf-break front, the rms finescale shear associated with the layers significantly exceeded the geostrophic shear.

An April 2002 follow-on cruise was organized to establish whether these motions were propagating internal waves. Both shipboard and lowered ADCPs were operated from the R/V *Melville*. In addition to CTD-sonar transects, a 30-h time series of currents and shear was obtained in the core of the Kuroshio near the island of Kyushu, Japan.

The shear structures were indeed found to be propagating, with both up and down-going internal wave motions present. Compared to the nearby open-ocean, the finescale (< 160 m) vertical shear variance is increased by a factor of 3 in the Kuroshio, and by a factor of 6 in the region between the shelf break and the Kuroshio. If energy dissipation indeed scales as shear variance squared (Gregg 1989), very high values of dissipation (over 30 times the open-ocean value) can be anticipated in this region. We conjecture that the geostrophic vorticity associated with the Kuroshio acts as a barrier, impeding the seaward propagation of internal waves generated at the shelf-break onshore of the Kuroshio front.

1. Introduction

The history of exploration of western boundary currents is intimately linked to the development of observational sensors and methods. With each advance, from ship-drift estimates through infrared satellite photography, new phenomena are revealed. Here we report the discovery of intense shear layers of 10-60 km horizontal extent and 10-50 m vertical scale in and under the Kuroshio. At issue is the role that these newly discovered structures might play in the larger scale dynamics of boundary current systems.

The initial observations were made using the new high-resolution Hydrographic Doppler Sonar System on the RV *Roger Revelle*, while participating in the Asian Seas International Acoustic Experiment (ASIAEX) in April 2000. Section 2 describes the cruises, instruments, and methods in more details. The spatially coherent finescale velocity and shear structures observed from transects across the Kuroshio during the ASIAEX 2000 cruise are described in section 3.

To determine if the shear features propagate vertically, a follow-on cruise (referred below as the Kyushu Cruise) was conducted in April 2002 to obtain time series in the core of the Kuroshio. Observations of propagation are presented in section 4. A dynamical interpretation is given in section 5.

The measured shear, when recast in terms of in terms of *scale dissipation* using the Gregg (1989) parameterization, suggests high levels of turbulent mixing shelfward and beneath the Kuroshio. The vertical component of vorticity associated with the Kuroshio is sufficient to affect the propagation of internal waves. For coastally generated waves, this could lead to the observed energy/shear build-up between the shelf and the core of the current, and possible trapping.

2. Data

The sites of the ASIAEX transect and the subsequent Kyushu time series (and transect) are shown in Figure 1a. Figure 1b shows the monthly mean sea-surface temperature in the area during April 2000, provided by the National Center for Ocean Research (Taiwan). The Kuroshio is seen as the warm water moving northward along the shelf break of the East China Sea, though the Tokara Strait, and along the East coast of Japan.

The R/V *Roger Revelle* conducted the April 2000 survey cruise of the ASIAEX field program in the East China

Corresponding author address: Luc Rainville, Scripps Inst. of Oceanography 9500 Gilman Dr., La Jolla, , CA 92093-0226
E-mail: luc@mpl.ucsd.edu

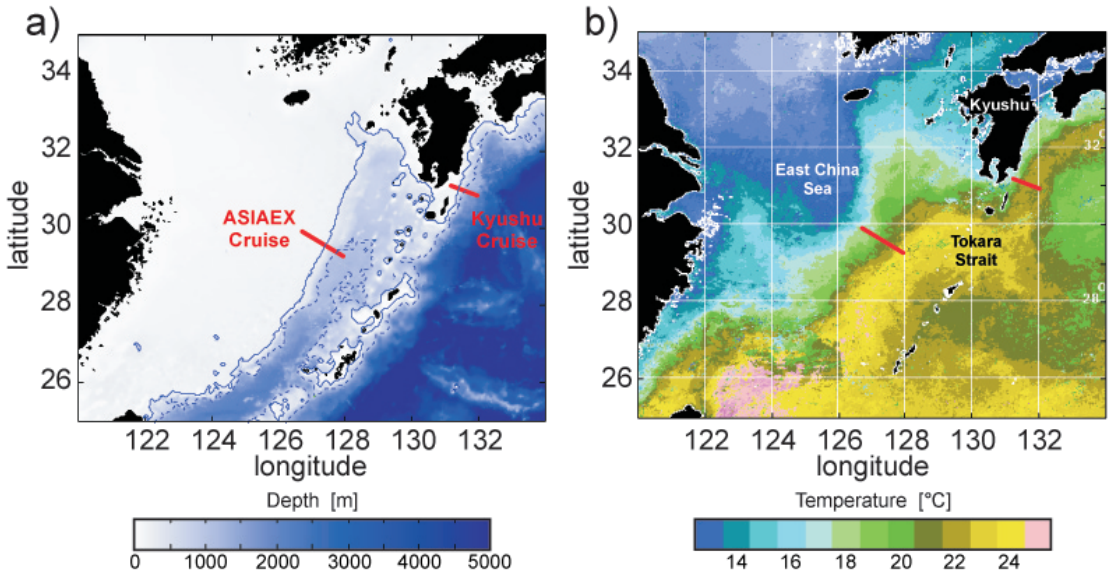

FIG. 1. (a) Bathymetry of the East China Sea and near Japan (Smith and Sandwell 1997). Land is shown in black, the solid blue line is the 200-m isobath and the blue dotted line is the 100-m isobath. Locations of the cruises are indicated. (b) April 2000 monthly mean of sea surface temperature, from satellite measurements. The Kuroshio is evident from the warm water flowing along the continental shelf.

Sea. The focus of the ASIAEX cruise was on geophysical observations on the continental shelf (Ramp et al. 2003). However, two Doppler sonar transects from the shelf to middle of the Kuroshio were obtained, along with a series of CTD stations. The bathymetry of the ASIAEX region is dominated by a broad and shallow continental shelf (100 meter deep) and a step-like shelf break. The Kuroshio flows parallel to the shelf break with velocities in excess of 1.5 m s^{-1}. Strong tidal currents are observed on the continental shelf, with flow directed normal to the shelf edge and amplitude occasionally over 0.4 m s^{-1}.

Direct measurements of the water velocity were obtained using the Hydrographic Doppler Sonar System (HDSS), a shipboard current profiler system designed and built at the Marine Physical Laboratory at SIO. It consists of synchronized 140 kHz and 50 kHz sonars, each with 4 beams directed 30° from vertical. Repeat sequence codes (Pinkel and Smith 1992) are transmitted from both sonars. The 50 kHz sonar pings every 2 sec and has a vertical resolution of about 13 m. Profiles are obtained to depths of 600-800 m. The 140 kHz sonar transmits at 0.6-sec intervals. With a vertical resolution of 4.5 m, depths of 200-300 m are achieved. Both sonars record time ensembles every 2 min.

In the April 2002 (Kyushu cruise) study area, the Kuroshio has just exited the East China Sea (Figure 1). It is still constrained against topography and is relatively narrow. The depth of the continental shelf along the cross-shelf line of the cruise is nearly constant (100 m) within 40 km from the coast. Then the bathymetry drops to over 1000 m in less than 15 km. In contrast to the East China Sea, the barotropic tides in this region are weak.

The Kyushu cruise was organized as an all-student cruise on the R/V *Melville*, funded by University of California Ship Funds. The cruise started with a 200-km, 13-station, hydrographic transect across the Kuroshio. The transect was followed by a 30-h yoyo station in the core of the current, to detect vertical propagation of the shear layers. Several stations were repeated around the frontal region.

A self-contained 150 kHz narrowband Doppler sonar (RDI) was used as a lowered acoustic Doppler current profiler (LADCP). An internally recording CTD (SBE19) was attached to the LADCP. At each station the instruments were lowered at 1 m s^{-1} to a depth of 1000 m. Each station lasted about 40 minutes. The setup of the LADCP is similar to that of Fischer and Visbeck (1993). The ensemble interval was set to 3 sec. Two pings per ensemble were recorded in Earth coordinates. The length of the acoustic pulse and the bin length were both 16m. Throughout the cast, the LADCP had a range of about 200m.

Absolute profiles of water velocity from the surface to 1200 m were obtained using the linear inverse method of Visbeck (2002). We used software available on the Web from Prof. M. Visbeck. (www.ldeo.columbia.edu/~visbeck/ladcp/). Navigation data, CTD measurements, and shipboard ADCP data were included in the inversion. During each station, the R/V *Melville* was allowed to slowly drift in the along-

shelf direction in order to maintain a small wire angle on the LADCP/CTD package. For the 30-h yoyo time-series, the ship was repositioned every 6 hours or so, after making about 10 profiles and drifting 15 to 20 km. During repositioning, the LADCP was out of the water. Velocity was also estimated by the shipboard 150 kHz ADCP, which provided data to depths of nearly 400m. 1-min ensembles were recorded from the shipboard ADCP during the entire cruise.

3. Spatially coherent shear structures: the ASIAEX cruise

Velocity and shear from two sections across the Kuroshio from the ASIAEX cruise in the East China Sea are presented in Figure 2. The top four panels show data during a continuous transit from the high-resolution 140 kHz sonar, smoothed by 9 m in the vertical and by 2 km in cross-shelf distance. Cross-shelf distance is calculated from the shelf break. Following the offshore transect, the ship repeated the section, stopping for CTD stations as it moved onshore. Data from the 50 kHz sonar collected during this section, smoothed by 20 m in the vertical and by 4 km in distance, are shown in Figures 2e,f. The locations of the CTD stations are marked on the upper axis of each panel. For reference, objectively mapped potential density contours, spaced by 0.25 kg m^{-3}, are plotted in Figure 2f.

The Kuroshio clearly dominates the velocity, and is directed almost entirely in the along-shelf direction (Figure 2b, positive is towards northeast, into the page). Cross-shelf velocities (Figure 2a, positive towards off-shore) are small in comparison. The vertical shear (9-m difference of velocity in Figures 2c,d, and 20-m difference in 2e,f) reveals a different picture. Alternating bands of high shear can be found below the core of the Kuroshio (where the isopycnals are level, under 500m) and appear to cross isopycnal surfaces. The velocity profiles have a structure very similar to those obtained by Winkel et al. (2002) in the Florida Strait and Toshihiro et al. (1994) in the East China Sea, suggesting that high-wavenumber velocities and shears seen in ASIAEX are common features of strong currents riding along the continental shelf.

Representative sonar-derived profiles of velocity and shear from the core of the Kuroshio are compared with density-derived estimates (based on the thermal wind equation, Gill (1982) in Figure 3. The black arrow on the top of Figure 2e,f indicates the position of this station, 46 km from the shelf break. The vectors in Figure 3a represent horizontal current in the cross- (x-) and along-shelf (y-) directions. Currents are plotted at 25 m intervals in depth, offset to the right with increasing depth. The gray arrows give low vertical wavenumber sonar-derived currents (k_z 1/200 m^{-1}). The along-shelf component (dotted gray line), i.e. the component perpendicular to the direction of the transect, is very similar to the geostrophic current profile (thick gray line) derived from the density field, assuming a level of no-motion of 1000 m. High-wavenumber sonar-derived velocity (1/150 $m^{-1} < k_z <$ 1/60 m^{-1}) is represented by the black arrows, which follow the same convention as the low-wavenumber velocity but are plotted at 5 m intervals and are multiplied by a factor 5 for clarity. In Figure 3b, the corresponding vertical shears (low wavenumber, high wavenumber, and geostrophic) are presented. Here, high-wavenumber shear is not multiply by the factor of 5, as in a). Note again the good agreement between low-passed sonar-derived shear and the geostrophic shear from the CTD. Also note that the high-wavenumber shear is of the same order of magnitude as the low-wavenumber shear.

The absence of the high wavenumber shear in the geostrophic signal is significant, given that the vertical resolution of the CTD is 5 m or better and that the lateral coherence scale of the shear is comparable to the CTD station spacing. Following ASIAEX, we concluded that these shears are ageostrophic, perhaps associated with propagating waves.

4. Variation in time: the Kyushu cruise.

The goal of the Kyushu cruise in 2002 was to obtain a time series in the Kuroshio to study the evolution of the shear structures. With only 3 days of ship time available, a single cross-shore section of the Kuroshio was initially obtained. A 30-h depth-time series was then collected at the maximum velocity point in the transect (nominally at 30° 45'N, 131° 45'E). Velocity and shear data from the 30-h yoyo station are shown in Figure 4, both smoothed by 1 h in time and 24 m in the vertical. The station consists of 4 separate deployments of the LADCP/CTD, each with 10 to 12 profiles from the surface to 1000 m. The deployments are separated by times when the ship repositions to its initial location (gaps in Figure 4). During each deployment the drift is almost exclusively in the along-shelf direction, following the Kuroshio. The water depth remains more or less constant at 1700 m. Intense along-shore and cross-shore shear is again seen. There is a considerable depth-time variability in the structure, presumably a mix of lateral advection and true time evolution. Note the velocity signature of an apparent baroclinic 12 h tide in the cross-shelf velocity.

Rotary vertical wavenumber spectra of the shear in the Kuroshio are presented in Figure 5. For linear near-inertial waves, clockwise rotation with increasing depth is associated with downward energy propagation (Leaman and Sanford 1975). The spectra are computed from the 42 LADCP profiles obtained during the yoyo station. Figure 5a shows the vertical shear spectra in three depth ranges: within the Kuroshio (0-400 m), around its base (400-800 m), and under (800-1200 m). In Figure 5b, the shear spectra are normalized by the mean buoyancy frequency squared to form a composite Froude spectrum (black lines).

The shape of the spectrum of Figure 5b is a good indication of the vertical scales resolved by the LADCP.

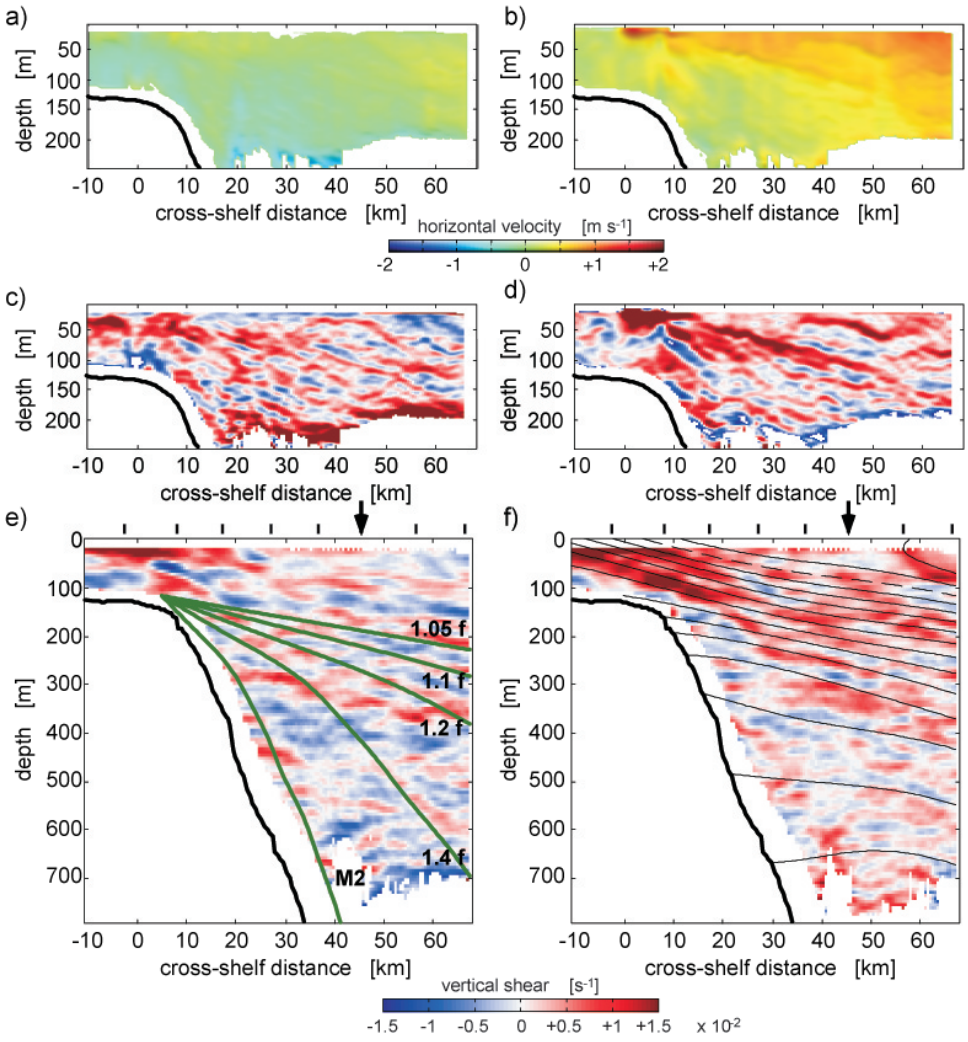

FIG. 2. Velocity and shear from two cross-shelf transects during ASIAEX. Panels a-d show data from the 140 kHz sonar during an underway transect [17 April 2000], and the 50 kHz data from a CTD section [18 April 2000] are shown (e) and (f). (a) Cross-shelf velocity. (b) Along-shelf velocity, in which the Kuroshio is evident. The corresponding vertical shears [(c) and (d)], and the deep cross-shelf (e) and along-shelf (f) shears, show strong alternating bands in and under the Kuroshio. In (e) and (f), the locations of the stations are shown on the top of each panel. For reference, rays for internal wave propagation in a quiescent medium are shown in (e) for different internal wave frequencies. Isopycnals are shown as black contours in (f). The $\sigma_0 = 24.0$ contour is indicated by the long-dashed line. The thick black line indicates the sea floor.

In the open ocean, shear (and Froude) spectra more-or-less follow the empirical Garrett-Munk spectrum, labeled here as GM (Garrett and Munk 1975; Gregg and Kunze 1991). Although its low-wavenumber level seems to be higher than GM by about a factor of 2, the measured spectrum rolls off at wavenumbers above 10^{-2} m^{-1}. Following Polzin et al. (2002), the LADCP Froude spectrum can be corrected for range averaging and interpolation. Since velocity measurements from Doppler sonars are effectively averages over the lengths of the transmitted pulse (Δz_t) and the bin (Δz_r), both 16 m, the net effect is a convolution of the true velocity profile with a triangle of base $\Delta z_t + \Delta z_r$. During the processing, each 3-sec ensemble is also interpolated to a fixed grid with spacing Δz_g =16 m, equivalent to another series of convolutions. The corrected vertical wavenumber spectrum is then:

$$S^{\text{corr}}(k_z) = \frac{S(k_z)}{T(k_z)}, \tag{1}$$

where $k_z = \lambda_z^{-1}$ is the vertical wavenumber in cycle per

meter (m^{-1}), and

$$T(k_z) = \text{sinc}^2(k_z\ \Delta z_t) \cdot \text{sinc}^6(k_z\ \Delta z_r) \cdot \text{sinc}^2(k_z\ \Delta z_g). \quad (2)$$

Because of differences in our processing, other corrections described in Polzin et al. (2002) are not applied here. The corrected spectra are believed to be accurate for wavelength larger than 50 m ($k_z \leqslant 2 \times 10^{-2}$ m^{-1}). The spectra apparently become noise dominated at smaller scales (Figure 5b).

Confidence intervals for the spectra of Figure 5 are calculated based on an estimate of effective number of degree of freedom. Since sequential velocity profiles are not completely independent, the effective number of degree of freedom are calculated from the autocorrelation as function of wavenumber and lag in time (or space) (D'Asaro and Perkins 1984). Systematic errors (such as the ones due to the transmit pulse and bin lengths, corrected above) are not represented in this error estimate.

As seen in Figure 5, there is no dominance of clockwise (CW) relative to counter-clockwise (CCW) rotation with depth. For the 30-h yoyo station, the energy of the component of CCW rotating shear represents 48% of total energy. However, propagating waves become apparent when looking at the individual components in the depth-time domain (Figure 6). To obtain Figure 6, the 30-h mean is removed from both horizontal velocity components, and the velocity perturbations are moved to an isopycnal-following frame (Alford and Pinkel 2000). In such a emphsemi-Lagrangian frame, the effect of vertical advection is minimized. Because of noise problems with the conductivity cell towards the end of the cruise, we use only temperature and the T-S relation to estimate density during the yoyo station. Differences between isopycnal- and isotherm-following coordinates are minimal given that the T-S relation displayed little variation over the duration of the time series.

Vertical shear is then computed for each profile and normalized by the 30 hr mean buoyancy frequency. By choosing Fourier components corresponding to only the positive (or negative) wavenumbers of $F(s_x + \mathrm{i}\ s_y)$, the Fourier transform in depth of complex shear for each profile, and performing an inverse Fourier transform, one obtains a depth-time map of the component rotating CCW (or CW) with depth.

This technique has been applied to the vertical shear of Figure 4, independently for each of the 42 velocity perturbation profiles. To account for instrument response, only wavenumbers smaller than 1/50 m^{-1} are used. The Fourier components are corrected by the squared root of the transfer function (Equation 2) prior to performing the inverse Fourier transform. The result, smoothed by 1 h in time, is shown in Figure 6. Although horizontal advection complicates the picture significantly, the propagation of the shear features with respect to the density field is clearly seen. The apparent time-continuity is significant, given that each of the vertical profiles is "polarization filtered" independently. A modest excess of upward relative to downward phase propagation is seen associated with CW rotation (Figure 6b), with the reverse tendency in the CCW record (Figure 6c). This suggests that a significant fraction of the shear variance is associated with internal waves whose intrinsic frequency is within a factor of two of the effective inertial frequency, where polarization effects become significant. [1]

5. Discussion: vorticity, wave refraction, and mixing

Why are these energetic waves found beneath and shoreward of the Kuroshio? We suspect that variations in the vertical component of vorticity associated with the presence of the strong geostrophic flow are refracting these waves significantly. Kunze (1985) derived the dispersion relation for low frequency internal waves propagating in geostrophic shear flow, finding that the background vorticity effectively modifies the planetary vorticity,

$$\begin{aligned} f_{\text{eff}} &= \left[f^2 + f\left(\frac{\partial V}{\partial x} - \frac{\partial U}{\partial y}\right) - \frac{\partial V}{\partial x}\frac{\partial U}{\partial y} - \frac{\partial U}{\partial x}\frac{\partial V}{\partial y} \right]^{1/2} \\ &\approx f + \frac{1}{2}\left(\frac{\partial V}{\partial x} - \frac{\partial U}{\partial y}\right) = f + \frac{\zeta}{2}. \end{aligned} \quad (3)$$

where U and V are the geostrophic velocities. The simplification comes from the approximation that the transverse shears, $|\partial U/\partial y|$ and $|\partial V/\partial x|$, and the strain components, $|\partial U/\partial x|$ and $|\partial V/\partial y|$, are much less than f. Kunze suggests that trapping and amplification can occur in regions of negative vorticity, where internal waves with intrinsic frequencies below the local planetary inertial frequency are confined. Similarly, regions of strong positive vorticity can act as barriers, reflecting internal waves of frequency $\omega < f_{\text{eff}}$.

It is instructive to examine a western boundary current in terms of its vorticity structure. Figures 7a,b show the along-shelf velocity and along-shelf shear for the transect across the Kuroshio during the Kyushu cruise, with the same smoothing as in Figure 2 (20 m in depth and 4 km in lateral distance). Cross-shelf distance is calculated from the shallowest CTD station, located about 25 km for the coast. For reference, the yoyo station described in the last section was located at a cross-shelf distance of about 65 km (indicated by the arrow). As in Figure 2, contours of potential density are plotted over the maps (spaced by 0.25 kg m^{-3}). The long-dashed line indicates the $\sigma_0 = 24.0$ contour. In contrast with ASIAEX (Figure 2), the Kuroshio is not directly against the continental shelf, but rather pushed offshore by a strong Eastward

[1] A reviewer suggested that an estimate of the intrinsic frequency of the waves might be made from the ratio of shear to strain at each vertical wavenumber, based on linear internal wave theory. While this practice is widely accepted, power spectra of the time series of strain are seen to have a pronounced peak at near inertial (or perhaps the sub-harmonic of the semi diurnal tidal) frequency. (Pinkel et al. (1987), Figure 10) Since inherently non-linear effects dominate the strain spectrum (and probably shear as well), interpreting shear-strain ratio from a linear perspective is ill-advised.

surface current, possibly caused by the observed steady winds from the west. Strong shears exist in the Kuroshio and in the region between the Kuroshio and the shelf break.

A map of effective inertial frequency, $f_{\text{eff}} = f + \frac{1}{2}\partial V/\partial x$ (here we assume $\partial V/\partial x \gg \partial U/\partial y$, particularly valid in the present case), is shown in Figure 7c. The horizontal gradient of along-shelf velocity is smoothed over 5 km. The vertical component of geostrophic vorticity associated with the Kuroshio front creates a wall of positive vorticity. The effective inertial frequency reaches $2f$, (formally) sufficient to reflect the semi-diurnal baroclinic tide! [2] Some of the assumptions of Kunze (1985) are clearly violated here ($\partial V/\partial x \sim f$) and it is unlikely that the present definition of f_{eff} properly describes the situation dynamically. However, the magnitude of the vorticity refraction must be very large in this region. Low frequency internal waves generated either offshore or onshore of the "wall" will be back-reflected towards their source (unless they can sneak beneath it). There is therefore a potential for trapping shelf-generated waves inshore of the wall.

Also apparent in Figure 7c are regions of intense negative vorticity, where f_{eff} is reduced to half its planetary value. The most intense regions are immediately beneath the Kuroshio front and immediately offshore of the wall. To the extent that shear features appear to extent right through these regions (7b), separate populations of locally confined sub-inertial waves are unlikely. [3]

As a measure of energy contained in high-wavenumbers, the observed finescale (50 λ_z 400 m) shear variance (both components) is plotted as function of cross-shelf distance in Figure 7d, together with the square of the observed mean (20 to 400-m) shear, and the square of the depth-averaged geostrophic shear. Quantities are calculated using all underway shipboard ADCP data from the Kyushu Cruise. Error bars for the shear variance are calculated from the χ^2 distribution based on the effective number of degrees of freedom (D'Asaro and Perkins 1984). The sonar-derived mean shear is seen to be co-located with the mean geostrophic shear. Peak observed values are larger than geostrophic, in part due to the finite (10-15 km) spacing of the CTD stations. The observed shear variance increases from offshore, where it approaches the open ocean levels, to onshore. Except in a small region near the Kuroshio front, the finescale shear variance is always greater than the mean shear squared. For offshore distances greater than 100 km, fine scale shear variance is more or less constant and very similar to the variance measured in the open ocean (along the R/V *Melville*'s previous transit from the Marshall Islands to Japan, for example). Within the Kuroshio, shear variance is close to a factor of 3 greater than the open ocean values. Further onshore, the ratio approaches a factor of 6. The build-up of shear variance between the Kuroshio and the shelf-break, is consistent with the vertical vorticity field of the Kuroshio, which can trap shelf-generated waves onshore.

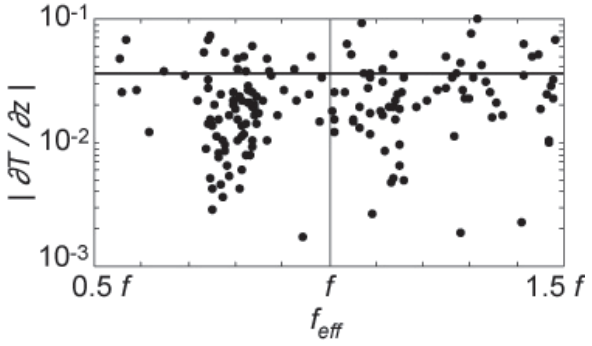

FIG. 8. Scatter plot of the absolute value of the temperature gradient as function of the effective inertial frequency, both averaged in 5 km by 20 m bins. The solid black line indicates the mean temperature gradient. Small temperature gradients (high strain) seem to occur predominantly at small f_{eff}.

The 5-m vertical temperature gradient profiles from 11 of the Kyushu CTD stations are plotted over the effective inertial frequency map in Figure 7c. Both in the Kuroshio and in the area between the shelf break and the Kuroshio, the temperature and conductivity profiles are dominated by stacking of high (negative) gradient regions (steps). The large gradient fluctuations indicate the presence of large-amplitude, small-scale internal waves, which deform the mean temperature profile. For reference, the depth-average vertical gradients for all profiles in the Kuroshio and near the shelf are smaller than 0.04 °C/m. There is a suggestion in Figure 7c that temperature gradient is correlated with effective inertial frequency. This is shown in Figure 8, where the absolute value of the temperature gradient, $\partial T/\partial z$, is plotted against effective inertial frequency. The solid black line indicates the mean gradient, averaged both in depth and over all stations. f_{eff} is averaged over bins of 5 km by 20 m centered around stations where the gradient is measured. Small values of temperature gradient correspond to large isotherm separations (high strain) and predominantly occur in areas of low effective inertial frequency. This is consistent with the trapping mechanism of Kunze (1985).

Spatially, the shear structures described here are reminiscent of the strong, east-dipping acoustic scattering layers observed from seismic reflection profiling in the front associated with the North Atlantic Current (Holbrook et al. 2003). These authors suggest that double

[2] The ray paths plotted in Figure 2e ignore the effect of the spatial variations in geostrophic vorticity. The magnitude of the observed variability is sufficient to make a M2 internal wave ($\omega \approx 1.9f$) effectively propagate at much shallower angles (e.g. along the path for $\omega = 1.2f$ if $f_{\text{eff}} = 1.6$).

[3] In comparing Figures 7b,c, it is clear that the horizontal scales of the vorticity field are smaller or comparable to the wave scales. The approximations made in the derivation of Equation 3 are clearly not justified. However, we feel that the Kunze (1985) propagation model can still serve as a useful guide in interpreting the observations.

diffusive processes are responsible for the scattering layers. Given the temperature and salinity profiles in both areas (salinity minimum around 400 m), double-diffusive processes are possible in the upper water column. These could possibly explain the temperature layering seen in the Kuroshio and between the Kuroshio and the shelf (Figure 7c). However, the observed high temporal variability, the cross-isopycnal propagation, and the strong shears seen in and beneath the Kuroshio are not suggestive of a double diffusion source.

There are no direct measurements of dissipation during either cruise. However a scale dissipation can be inferred from sonar-derived estimates of finescale shear variance (Gregg 1989; Polzin et al. 1995; Sun and Kunze 1999). The original Gregg (1989) parameterization requires that shear be resolved to 10 m vertical scales.

Unfortunately, direct estimates of shear variance at scales smaller than 50 m are not possible with lowered-ADCPs (Polzin et al. 2002). The *Melville*'s shipboard sonar also appears to have poor resolution during the Kyushu cruise. This is demonstrated in Figure 9, where vertical wavenumber Froude spectra are presented for stations offshore, within the Kuroshio, and between the Kuroshio and the shelf. Data from the shipboard ADCP in the depth range 20 to 400m were used. For comparison, Froude spectra within the Kuroshio are also shown using the R/V *Roger Revelle*'s 50 kHz sonar (20-400m) and from the 140 kHz sonar (20 to 210 m). Here, the CCW and CW components, which show no significant differences, have been summed. The GM spectrum is also shown. The shear variance build-up in and inshore of the Kuroshio is evident.

The RDI shipboard ADCP used during the Kyushu cruise (thick lines) appears to underestimate vertical shear for vertical wavenumbers larger than 1/50 m^{-1}. During this cruise, the RD sonar transmitted a pulse of duration equal to the depth-average bin ($\Delta z_t = \Delta z_r$). Effectively, this smoothes the velocity profiles and reduces high-wavenumber shear. The 50 and 140 kHz sonars on the R/V *Roger Revelle* use repeat sequence code and different processing, resolving shear to higher wavenumbers. Unfortunately the cross-shelf sections of the ASIAEX cruise do not extend fully across the Kuroshio.

However, Polzin et al. (2002) find that 50-m shear measured by lowered-ADCP (with a response correction) can be used to infer dissipation to within a factor of 3-4 using an adjusted version of the Gregg (1989) parameterization. For both the ASIAEX and the Kyushu cruises, applying their implementation of Gregg (1989) on 50-m shear (from shipboard and lowered-ADCP) leads to scale dissipation levels between 0.5 and 1.5?10-8 W kg^{-1} in the Kuroshio.

Winkel et al. (2002) present direct measurements of dissipation in the Florida Strait, where bands of high mixing are associated with bands of high shear. They report an increase in shear variance in the Florida Strait (1-4 times the open ocean counterpart) similar to the observed increase in the Kuroshio. They also find that the

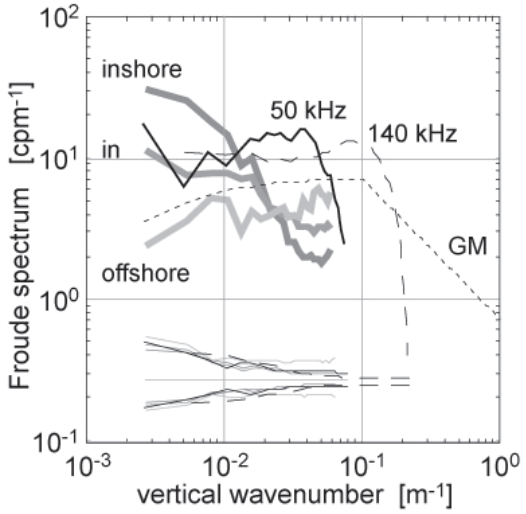

FIG. 9. Froude spectra of vertical shear from 20 to 400 m. The thick gray lines are from the shipboard ADCP (RDI) during the Kyushu cruise: inshore of the Kuroshio, in the Kuroshio, and offshore. The spectra in the Kuroshio during ASIAEX are shown by the thin black lines: from the HDSS 50 kHz sonar in the same depth range in solid, and from the 140 kHz in the range 15 to 210 m in dashed. The dotted line is the GM spectrum.

Gregg 10-m shear parameterization correctly predicts the observed value of dissipation. However, given the absence of ground truth direct dissipation measurements, we focus here on the spatial variability of the shear. If it is assumed that dissipation varies as shear variance squared, the factor of 2-3 increase in shear variance in the Kuroshio relative to the open ocean suggests 4 to 9 times more dissipation in the current than offshore. In the area between the Kuroshio front and the shelf break, the observed build-up of shear leads to scale dissipation levels 30-40 times greater than in the open ocean. The effect of these elevated dissipations on the dynamics of the Kuroshio warrants further study.

6. Conclusions

We report the discovery of intense, spatially coherent shear layers extending from the shelf edge through and beneath the Kuroshio. Initial observations (ASIAEX) indicated that the sonar-derived high-wavenumber rms shear in the Kuroshio is of the same order of magnitude as the geostrophic, low-wavenumber shear, as calculated from both CTD stations separated by 10 km and from shipboard Doppler sonar. Measurements from the follow-up Kyushu cruise suggested that the shear is associated with propagating low frequency internal waves. The vertical component of geostrophic vorticity is of order f, with a distinct spatial signature. Vorticity variability is sufficient to strongly refract low-frequency internal waves, perhaps trapping shelf-generated waves shore-

ward of the Kuroshio. The vertical temperature profile is "steppy", with the most pronounced variability in regions where the effective inertial frequency f_{eff} differs significantly from f.

The near-shelf increase in shear variance corresponds to an increase in dissipation of a factor of 40 relative to open ocean values, provided that the currently accepted parameterization linking microscale dissipation and finescale shear (Gregg 1989) is valid.

The internal wave generation mechanisms are not presently known. Internal waves can be generated by the Kuroshio itself (geostrophic adjustment), by its interaction with the coast, and by independent shelf processes. Because of the strong geostrophic vorticity, even the semi-diurnal internal tide might become effectively near-inertial. In the East China Sea, the barotropic tide, interacting with the shelf, is a likely source of internal waves. However the tide is very small in the region of the Kyushu cruise (TPXO models, Egbert and Erofeeva (2002). Modeling efforts, combined with intensive, long duration observations, are needed to further identify wave generation mechanisms and quantify interactions with the larger scale flows.

Acknowledgements. Eric Slater, Mike Goldin, Mai Bui, Chris Neely, and Lloyd Green designed and built the Hydrographic Doppler Sonar System, and we acknowledge their contribution and commitment to this work. We thank the Captain Desjardins, Captain Murline, and crews of the R/V *Roger Revelle* and R/V *Melville* for their excellent support. We are grateful to the UC Ship Fund Committee for supporting the Kyushu cruise, as well to the SIO Graduate Department . Benjamin Hodges, Yueng Lenn, Joseph Martin, and Andrey Shcherbina volunteered to participate in the Kyushu cruise. Dr. Teresa Chereskin helped in processing the Kyushu cruise shipboard ADCP data. We also thank the reviewers for their comments on the manuscript, the ASIAEX principal investigators and the Office of Naval Research.

REFERENCES

Alford, M. and R. Pinkel, 2000: Observations of overturning in the thermocline: the context of ocean mixing. *J. Phys. Oceanogr.*, **30**, 805–832.

D'Asaro, E. and H. Perkins, 1984: A near-inertial internal wave spectrum for the Sargasso Sea in late summer. *J. Phys. Oceanogr.*, **14**, 489–505.

Egbert, G. and S. Erofeeva, 2002: Efficient inverse modeling of barotropic ocean tides. *J. Atmos. Oceanic Technol.*, **19**, 183–204.

Garrett, C. and W. Munk, 1975: Space-Time Scales of Internal Waves: A Progress Report. *J. Geophys. Res.*, **80**, 291–297.

Gill, A., 1982: *Atmosphere-Ocean Dynamics.*. Academic Press, 662 pp. pp.

Gregg, M., 1989: Scaling turbulent dissipation in the thermocline. *J. Geophys. Res.*, **94**, 9686–9698.

Gregg, M. and E. Kunze, 1991: Shear and strain in Santa Monica basin. *J. Geophys. Res.*, **96**, 16709–16719.

Holbrook, W., P. Páramo, S. Pearse, and W. Schmitt, 2003: Thermohaline fine structure in an oceanic front from seismic reflection profiling. *Science*, **301**, 831–824.

Kunze, E., 1985: Near-inertial wave propagation in geostrophic shear. *J. Phys. Oceanogr.*, **15**, 544–565.

Leaman, K. and T. Sanford, 1975: Vertical energy propagation of inertial waves: a vector spectral analysis. *J. Geophys. Res.*, **80**, 1975–1978.

Pinkel, R., A. Plueddemann, and R. Williams, 1987: Internal waves observations from FLIP in MILDEX. *J. Phys. Oceanogr.*, **17**, 1737–1757.

Pinkel, R. and J. Smith, 1992: Repeat-Sequence Coding for Improved Precision of Doppler Sonar and Sodar. *J. Atmos. Oceanic Technol.*, **9**, 149–163.

Polzin, K., E. Kunze, J. Hammond, and E. Firing, 2002: The finescale response of lowered ADCP velocity profiles. *J. Atmos. Oceanic Technol.*, **19**, 205–224.

Polzin, K., J. Toole, and R. Schmitt, 1995: Finescale parameterizations of turbulent dissipation. *J. Phys. Oceanogr.*, **25**, 306–328.

Ramp, S., J. Lynch, P. Dahl, C.-S. Chiu, and J. Simmen, 2003: Program fosters advances in shallow-water acoustics in Southeastern Asia. *EOS Trans. AGU*, **84**, 361,367.

Smith, W. and D. Sandwell, 1997: Global seafloor topography from satellite altimetry and ship depth soundings. *Science*, **277**, 1957–1962.

Sun, H. and E. Kunze, 1999: Internal wave-wave interactions. Part II: spectral energy transfer and turbulence production. *J. Phys. Oceanogr.*, **29**, 2905–2919.

Toshihiro, S., Y. Hiroyuki, I. Haruo, and O. Akihiko, 1994: Observations of velocity profiles of the Kuroshio. *Proceedings of the China-Japan Joint Symposium of the Cooperative Research on the Kuroshio*, China Ocean Press, 112–120.

Visbeck, M., 2002: Deep velocity profiling using lowered acoustic Doppler current profiler: bottom track and inverse solution. *J. Atmos. Oceanic Technol.*, **19**, 794–807.

Winkel, D., M. Gregg, and T. Sanford, 2002: Patterns of shear and turbulence across the Florida Current. *J. Phys. Oceanogr.*, **32**, 3269–3285.

Generated with ametsocjmk.cls.

Written by J. M. Klymak

mailto:jklymak@ucsd.edu

http://opg1.ucsd.edu/ jklymak/WorkTools.html

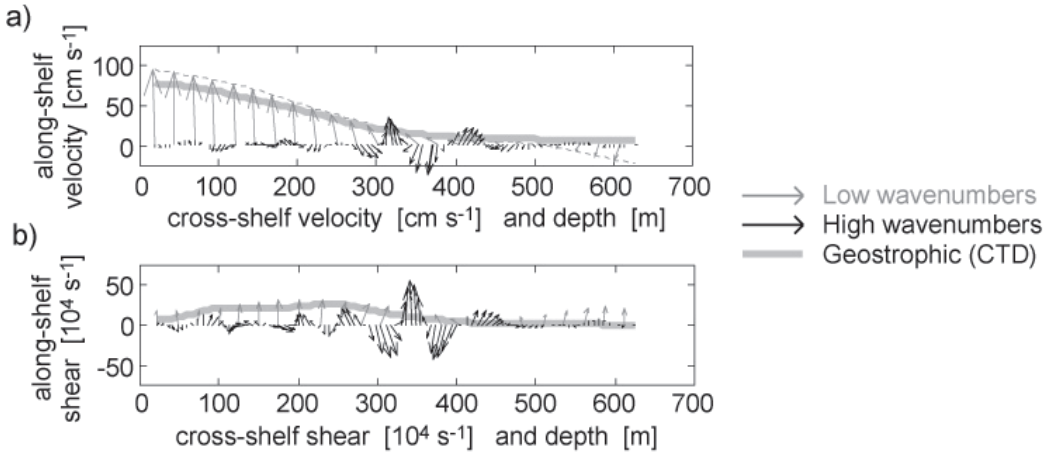

FIG. 3. (a) Horizontal velocity vectors as function of depth at a station in the Kuroshio (whose location is shown in Figure 2). The arrows represent horizontal currents (along-shelf and cross-shelf) offset to the right with increasing depth. The gray arrows show low vertical wavenumber currents (λ_z >200 m), very similar to the geostrophic currents derived from the CTD data, plotted as the thick gray line. In black are the high-wavenumber currents (150 > λ_z > 60 m), multiplied here by a factor 5. (b) Vertical shear profiles, plotted as in (a), showing the geostrophic (thick gray line), low-wavenumber (gray arrows), and high-wavenumber (black arrow) shear.

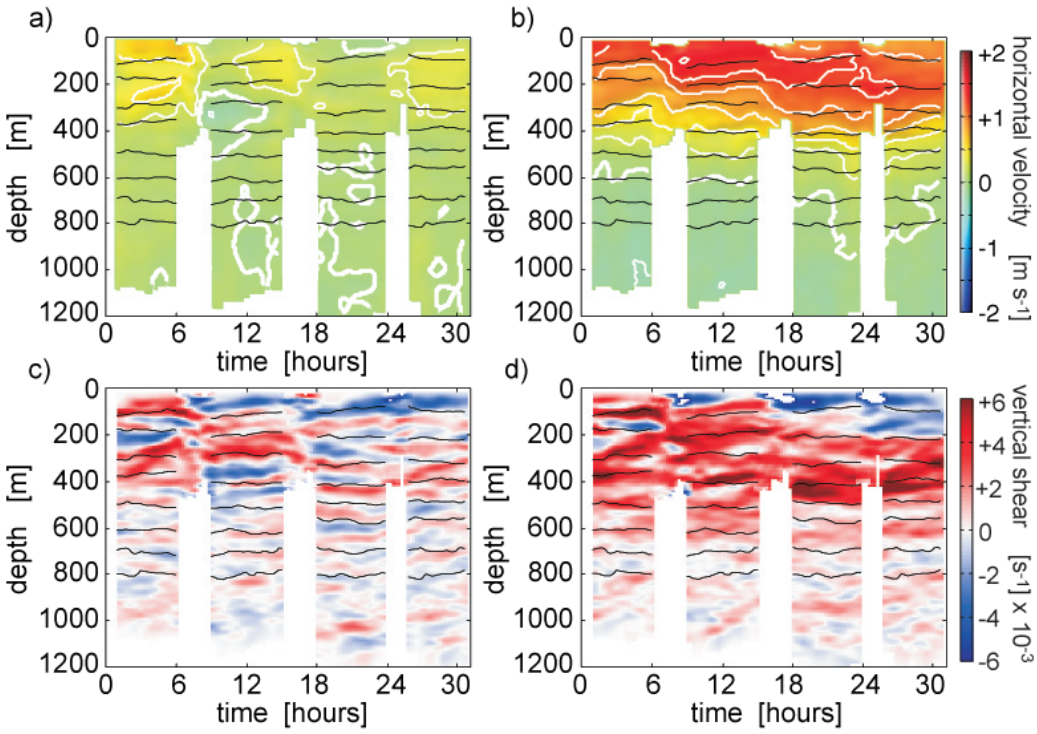

FIG. 4. Yoyo station in the core of the Kuroshio. (a) Cross-shelf velocity. (b) Along-shelf velocity. Velocity contours (separated by 0.25 m/s) are shown in white, with the zero isotach made thicker. The vertical shear of the cross-shelf (c) and along-shelf (d) velocity components is also shown. Here again, alternating bands of high shear are seen in and under the Kuroshio. The isopycnals whose mean depths are separated by 100m are shown as black contours.

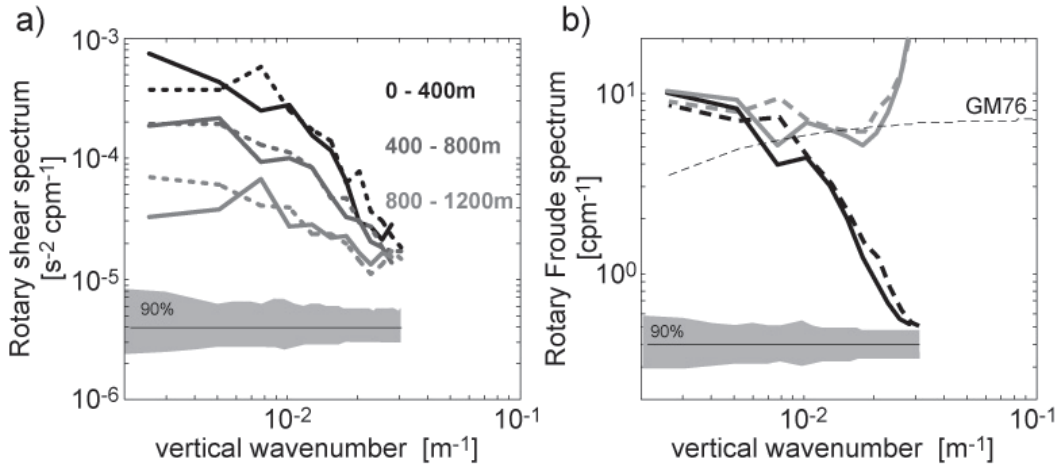

FIG. 5. (a) Rotary shear spectra from the L-ADCP for three depth ranges. The CCW and CW components are shown by the solid and dotted lines respectively. There is no clear dominance of one rotating component. All depths can be combined together when computing the Froude spectrum (b). GM is shown as the thin dotted line. In (b), the spectrum with corrected response described in the text is plotted in gray.

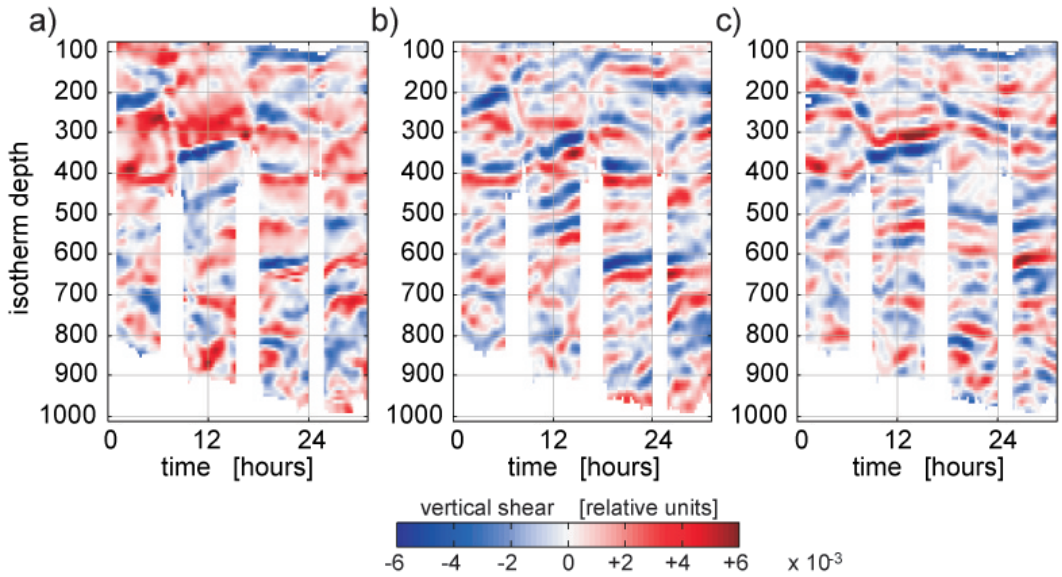

FIG. 6. Depth-time maps of cross-shelf vertical shear for the 30-h yoyo station. (a) Cross-shelf shear fluctuations, normalized by N and moved to an isopycnal frame. The components rotating CW (b) and CCW (c) with depth are separated by doing an inverse Fourier transform on respectively the positive and negative wavenumbers of the rotary spectrum. The shear is normalized by the buoyancy frequency and moved to isopycnal coordinates. While lateral advection is important, there is a dominance of upward phase propagation in (b) and downwards in (c).

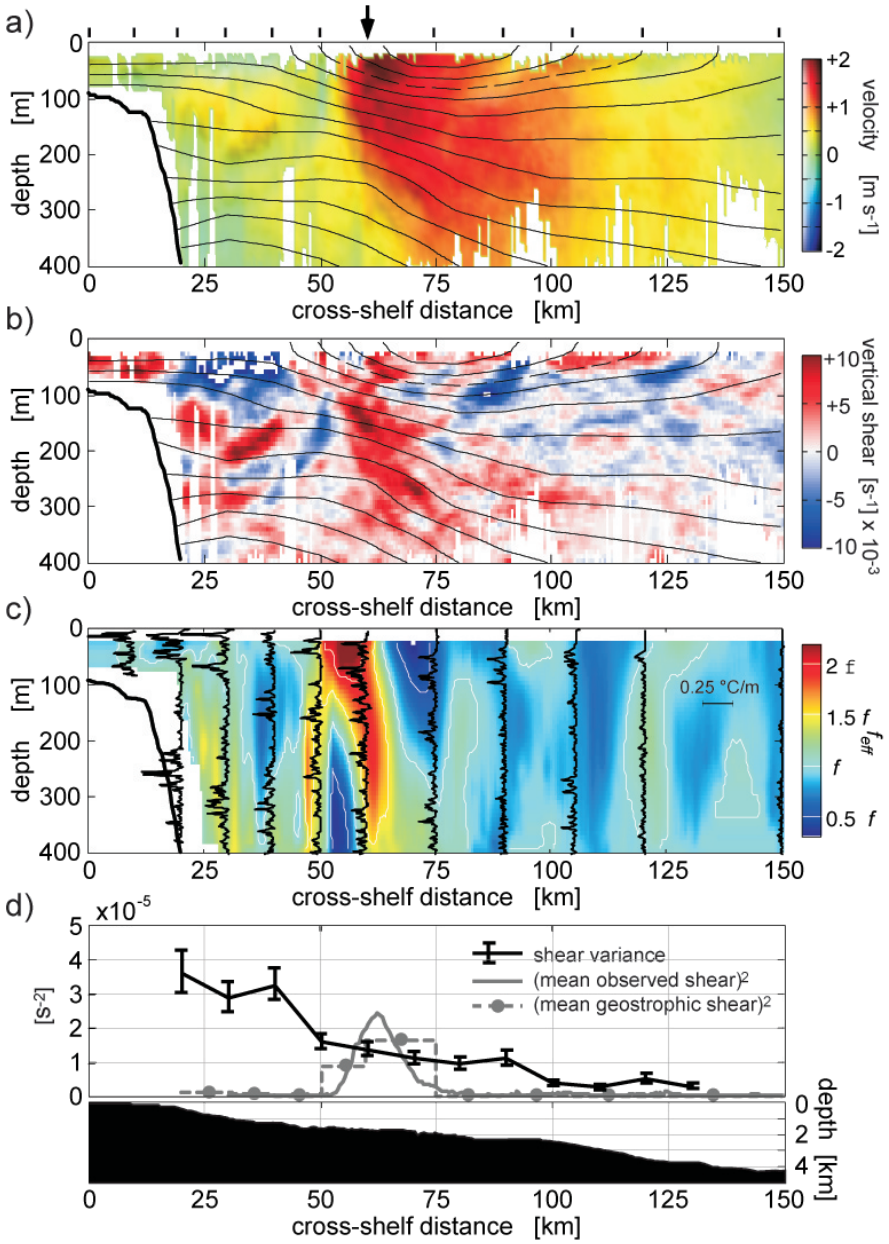

FIG. 7. Section across the Kuroshio during the Kyushu cruise showing (a) the along-shelf velocity, (b) the along-shelf vertical shear. The isopycnals are shown as black contours and the stations locations are indicated on the top panel (arrow shows yoyo station). (c) Effective inertial frequency along with the temperature gradient profiles at the location of each station. (d) The black line shows shear variance versus distance based on shipboard ADCP (20 to 400-m depth range, $\lambda_z \leqslant 50$ m). The solid gray line is the square of the observed mean along-shelf shear, and the dotted gray line is the square of the 25-400-m depth-averaged geostrophic shear (computed between pairs of stations). Depth is plotted on the lower panel.